THE JOURNAL OF PHYSICAL CHEMISTRY C

Article

pubs.acs.org/JPCC

Coherent Manipulation of Polarization in Mixed-Valence Compounds by Electric Pulse via Landau–Zener Transitions

Andrew Palii,*[,†] Boris Tsukerblat,*[,‡] Juan Modesto Clemente-Juan,[§] and Eugenio Coronado[§]

[†]Institute of Applied Physics, Academy of Sciences of Moldova, Kishinev, Moldova

[‡]Ben-Gurion University of the Negev, Beer-Sheva, Israel

[§]Instituto de Ciencia Molecular, Universidad de Valencia, Paterna, Spain

ABSTRACT: In this contribution, we predict and theoretically investigate the effects of the electric field pulse in mixed valence (MV) dimers. These systems exhibit bistability with a large internal dipole moment mediated by the itinerant electron trapped by the vibronic coupling. In this sense, they are similar to single molecular magnets (SMMs) that are bistable systems possessing large long-living magnetization and exhibiting Landau–Zener (LZ) transitions. We propose a scheme for a controllable LZ tunnelling in MV systems that provides also a possibility to control the dipole moment of a dimeric MV unit. It is supposed that the static electric field initially polarizes the system, and then the unit is subjected to a short electric pulse controlling the LZ transitions. The model includes the vibronic pseudo Jahn–Teller (JT) coupling in a MV dimeric system belonging to Class II in Robin and Day classification. We elucidate the main factors controlling coherent nonadiabatic LZ tunneling between the low-lying vibronic levels induced by a short pulse of the electric field. The transition probabilities and consequently polarization induced via the LZ transitions are shown to be dependent on both the time of the pulse and total spin of the cluster. We have suggested to employ the electric field pulse as a tool for the direct observation of the tunneling splitting through the coherent LZ transitions. The magnetic MV systems in which the double exchange is operative are shown to provide a possibility to control electric polarization through the spin-dependent LZ tunneling by applying an additional static magnetic field. The ability of MV systems to change electric polarization in a controllable manner seems to be significant for potential applications.

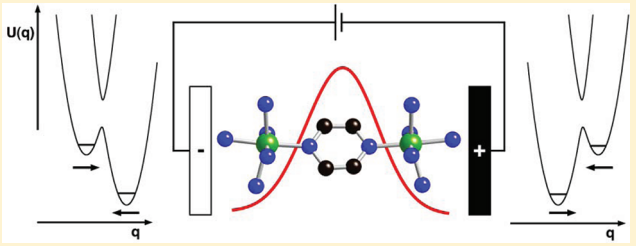

1. INTRODUCTION

Single-molecule magnets (SMMs)[1−6] have been the most promising spin systems to date for observing quantum phenomena such as Landau–Zener (LZ) tunneling within their spin ground states. It was discovered that the Mn_{12} acetate molecule (Mn_{12}) exhibits slow relaxation of magnetization at low temperature due to the presence of the barrier for reversal of magnetization arising from the magnetic anisotropy. Under this condition a single molecule behaves like a tiny magnet and being magnetized by an applied field is able to retain magnetization for a long time. Presently, many classes of SMMs are discovered, and the concept of single-molecule magnetism is well developed.[1] Nowadays this field remains topical due to a possibility of the design of the memory storage devices of molecular scale, quantum bits (qubits) and study of the fundamental aspects of quantum effects in the nanoscopic objects. Study of SMMs[1,7−12] revealed a possibility to observe the LZ tunneling[13] that is one of the most interesting quantum phenomena in the nanoscale systems.

In this article, we propose a scheme for a controllable LZ tunneling in a molecule that has a large dipole moment and a barrier separating two opposite directions of polarization. To achieve this goal, it is worthwhile to employ binuclear mixed valence (MV) clusters, the molecular entities that are composed of the two metal ions in different oxidation degrees and therefore containing an "extra" electron (or hole) that can travel between the metal ions.[14−19] If the barrier is large enough, this molecule can have a long relaxation time for reorientation of the internal dipole moment and consequently exhibits bistability. In this sense, such bistable dipole systems are similar to SMMs exhibiting a slowly relaxing magnetic moment. As distinguished from SMMs in which the barrier for the magnetization reversal is caused by the anisotropic magnetic interactions, the MV dimers exhibit a barrier for the reversal of the electric dipole moment that is created by the pseudo Jahn–Teller (JT) vibronic interaction. It is notable also that in SMMs the LZ transitions are induced by a time-dependent magnetic field, whereas in MV clusters such transitions are expected to be caused by a time-dependent electric field.

We will assume that the MV system is initially polarized by a static electric field and then is subjected by the action of the time-dependent electric field which represents a pulse of the Gaussian form added to the static electric field (as schematically shown in Figure 1). The static electric field induces parallel alignment of the electric dipole moments, while the electric field pulse is expected to partially destroy this alignment through the

Received: November 16, 2011
Revised: January 24, 2012
Published: January 24, 2012

   dx.doi.org/10.1021/jp211057e | J. Phys. Chem. C 2012, 116, 4999–5008

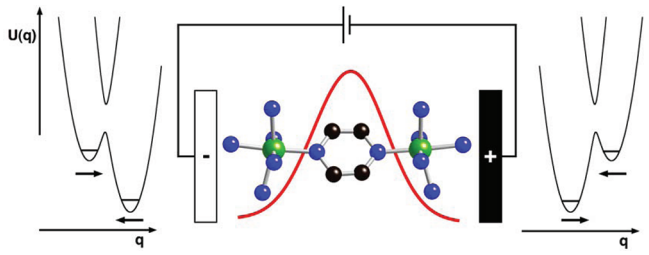

Figure 1. Schematic image of a MV dimer (conventionally, Creutz–Taube ion) subjected to a combined action of a static electric field (applied along the molecule) and a pulse of the electric field directed along the axis of polarization. Arrows indicate the directions of the dipole moment corresponding to the minima of the lower sheet of the adiabatic potential.

LZ transitions, with the latter effect being dependent on the sweep rate of the electric field at the leading and the trailing edges of the pulse. As distinguished from the conventional studies of MV compounds based on the well-elaborated Stark spectroscopy[20−24] that exploits the ability of the applied electric field to significantly change the intervalence band, consideration of the LZ tunneling effects in MV compounds seems to be an unexplored area, and the present article represents the prediction and a first step toward the theoretical description of this phenomenon.

The model for a MV dimer used in this article is represented by a "truncated" two-state system that has a quite common interest in physics and chemistry,[25] and in particular, the two-site vibronic systems became a subject in the prospects for molecular electronics.[26] That is why the tunneling splitting that is an inherent property of the vibronic systems (JT tunneling[27] in molecules, inversion splitting in ammonia, etc.) has been intensively studied. To the best of our knowledge, only the indirect information about the tunneling splitting is presently available. In this paper, we show that the proposed scheme based on the application of the electric field pulse can be employed as a tool for the direct observation of the tunneling splitting through the coherent LZ transitions. A similar scheme was recently proposed for a SMM subjected by a magnetic pulse.[28]

Along with the simplest one-electron MV dimer belonging to the Robin and Day Class II,[16] we will consider a MV dimer containing localized spins coupled to the itinerant electron through the double exchange[29] (see also reviews[16]). It was shown that the double exchange tends to stabilize the ferromagnetic state of a MV pair.[29] For example, one can mention that a recently discovered high-spin ground state via electron delocalization was recently found in MV imidazolate-bridged divanadium complexes.[30] In MV pairs belonging to the Class II,[16] the valence electron at low temperature is trapped, and the double exchange is significantly suppressed. It will be shown, however, that under some conditions in the presence of the electric field pulse the double exchange becomes operative even at zero temperature due to the spin-dependent LZ tunneling that changes the electric dipole moment of a MV cluster. It will be demonstrated that the response of the system to the time-dependent electric field can be tuned by applying a static magnetic field. A possibility to achieve a controllable dipole moment in the nanoscale objects through the coherent LZ tunneling seems to be attractable for various possible technological applications, particularly for the creation of qubits and quantum logical gates.[31] New fascinating perspectives are related to the transport phenomena at the molecular level[32,33] that are in the core of the rapidly developing field of molecular spintronics.

2. VIBRONIC MODEL OF A MIXED-VALENCE DIMER, TUNNELING SPLITTING

Let us first consider as the simplest example a MV dimer comprising one extra electron delocalized over two cores A and B. Within the basic vibronic model proposed by Piepho, Krausz, and Schatz (PKS model),[15−17,27] the instantly localized mobile electron is assumed to interact with the independent full-symmetric ("breathing") modes Q_A and Q_B located on the sites A and B. The out-of phase mode $Q_- = (Q_A - Q_B)/\sqrt{2} \equiv Q$ is relevant to the vibronic problem in the whole system, while the in-phase mode $Q_+ = (Q_A + Q_B)/\sqrt{2}$ can be eliminated by a shift transformation of the Q_+ coordinate.[15] The total Hamiltonian of a MV dimer with equivalent spinless sites A and B can be represented as

$$H = \left(\frac{P^2}{2M} + \frac{1}{2}kQ^2\right)\mathbf{I} + \frac{l}{\sqrt{2}}Q\boldsymbol{\sigma}_Z + B\boldsymbol{\sigma}_X \tag{1}$$

In eq 1, P is the kinetic moment operator; M is the effective mass of the out-of-phase vibration, $B = \langle\varphi_A|\hat{h}|\varphi_B\rangle$ is the electron transfer integral ($\hat{h}$ is the one-electron part of the Hamiltonian); l is the vibronic coupling parameter; $\boldsymbol{\sigma}_Z$ and $\boldsymbol{\sigma}_X$ are the Pauli matrices defined on the basis of the localized orbitals $\varphi_A(r) = \varphi_A(r - R_A)$, $\varphi_B(r) = \varphi_B(r - R_B)$, and $\mathbf{I}$ is the unit matrix.

In terms of the dimensionless variables q and p one obtains

$$H = \hbar\omega\left[\frac{1}{2}\left(q^2 - \frac{\partial^2}{\partial q^2}\right)I + \lambda q\boldsymbol{\sigma}_Z + \beta\boldsymbol{\sigma}_X\right] \tag{2}$$

where

$$q = \sqrt{M\omega/\hbar}\,Q, \quad p = (M\hbar\omega)^{-1/2}P,$$
$$\lambda = (2\pi M\omega^3)^{-1/2}l, \quad \beta = B/(\hbar\omega)$$

are the dimensionless coordinate, linear momentum, vibronic coupling, and transfer parameters, respectively. All energies are measured in $\hbar\omega$ units (ω is the vibrational frequency). Applying a shift transformation to the vibrational coordinate

$$q' = q + \lambda, \quad q'' = q - \lambda \tag{3}$$

one can present the Hamiltonian as follows

$$H = \hbar\omega\begin{pmatrix} & \varphi_A & & \varphi_B \\ & -\frac{\lambda^2}{2} + \frac{1}{2}\left(q'^2 - \frac{\partial^2}{\partial q'^2}\right) & & \beta \\ & \beta & & -\frac{\lambda^2}{2} + \frac{1}{2}\left(q''^2 - \frac{\partial^2}{\partial q''^2}\right) \end{pmatrix} \tag{4}$$

In the case of uncoupled sites ($\beta = 0$), the adiabatic potentials of the dimer represent two intersecting parabolas with the minima at $q = \pm\lambda$ corresponding to the localization of the extra electron on the sites A and B, respectively, and the

dx.doi.org/10.1021/jp211057e | J. Phys. Chem. C 2012, 116, 4999−5008

energy pattern comprises two sets of equivalent harmonic oscillator levels as shown in Figure 2

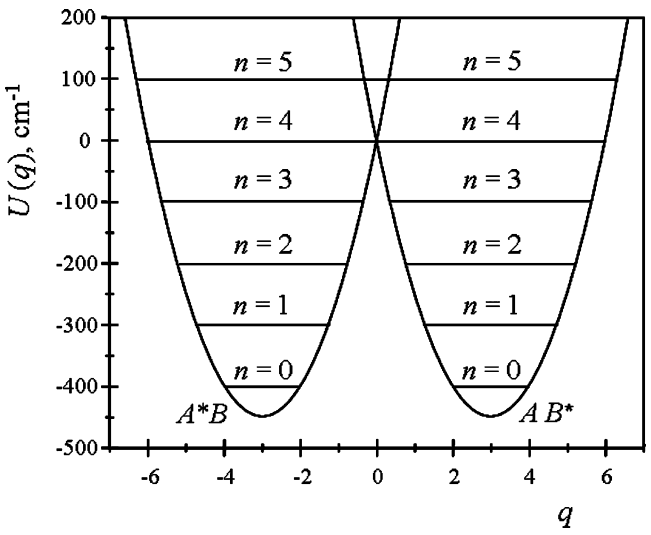

Figure 2. Adiabatic potential wells and energy pattern of the one-electron MV dimer: $\beta = 0$, $\lambda = 3$, $\hbar\omega = 100$ cm^{-1}.

$$\varepsilon_A(n) = \varepsilon_B(n) = \hbar\omega\left(-\frac{\lambda^2}{2} + n + \frac{1}{2}\right) \tag{5}$$

The corresponding eigenvectors are the products of the electronic orbitals φ_A, φ_B and the harmonic oscillator wave functions with the equilibrium positions shifted to minima of the adiabatic potential

$$\chi_n^A(\mathbf{r}, q) = \varphi_A(\mathbf{r})\Phi_n(q + \lambda),$$
$$\chi_n^B(\mathbf{r}, q) = \varphi_B(\mathbf{r})\Phi_n(q - \lambda) \tag{6}$$

The inclusion of the electron transfer ($\beta \neq 0$) results in the pseudo JT mixing of the two levels so that the adiabatic potential consists of the two sheets

$$U_\pm(q) = \hbar\omega(q^2/2 \pm \sqrt{\lambda^2 q^2 + \beta^2}) \tag{7}$$

The upper sheet $U_+(q)$ has a minimum at $q = 0$. Providing weak vibronic coupling or/and strong transfer $\lambda^2 < |\beta|$, the lower sheet $U_-(q)$ has the only minimum at $q = 0$ so that the system proves to be fully delocalized even at all temperatures and belongs to the so-called Class III MV compound according to the Robin and Day classification scheme.[14−16] In the opposite case of strong coupling $\lambda^2 > |\beta|$ the $U_-(q)$ represents a double-well sheet with the maximum at $q = 0$ and two minima shifted at the points

$$q_m^\pm = \pm\sqrt{\lambda^2 - \beta^2/\lambda^2} \tag{8}$$

If the minima are deep enough to allow for the existence of the discrete quantum levels and the depth of the minima are comparable with the thermal energy, such a system behaves as localized at low temperatures and delocalized at high temperatures belonging thus to the Class II in Robin and Day nomenclature. Finally, for $\lambda^2 \gg |\beta|$ the extra electron is strongly trapped in a deep minimum, and the system can be assigned to the fully localized Robin and Day Class I.

Here we focus on the Class II systems assuming that the minima of $U_-(q)$ (Figure 2) are deep enough to ensure localization, but at the same time the electron transfer is expected to produce a relatively weak (in the sense indicated below) tunneling splitting. There is a great variety of MV compounds ranging from fully localized (weakly coupled) Class I systems to fully delocalized (strongly coupled) Class II ones.[18,19] In between these two limits we face numerous systems belonging to intermediate Class II in which the extent of the delocalization changes quite continuously from the weakly coupled systems lying on the borderline between Classes I and II to the almost delocalized borderline Class II/III systems. More detailed classification of the Class II systems is discussed in ref 18 where this class is subdivided into the weakly coupled Class IIA (more close to the Class I) and more strongly coupled Class IIB that is closer to the Class III.

To illustrate the relevance of these specific requirements to the MV systems so far obtained one can appeal to the most studied compounds originated from the classic Creutz−Taube ions.[18,19,24] In these complexes, the interaction in Ru^{II}/Ru^{III} pairs occurs through the delocalization of the extra electron across the different conjugated bridging ligands L. The position and the intensity of the intervalence optical absorption band allow us to estimate the electronic coupling parameters (β) that are given in ref 19 for a series of $[(NH)_5Ru(\mu\text{-}L)Ru[(NH)_5]^{5-}$ complexes with different bridging ligands L (see Table 1 in ref 19). Taking into account the estimations of the frequencies of the "breathing" (PKS) modes from ref 24 (100 ± 300 cm^{-1}), one can estimate the vibronic coupling parameters λ in our model and estimate also the tunneling splitting δ. In particular, for the Class II compounds the position of the maximum of the intervalence band (Marcus reorganization energy) $\Omega_m = 2\lambda^2\omega$ is directly related to the vibronic coupling parameter λ. Such a kind of analysis of the data for the five Ru^{II}/Ru^{III} complexes in ref 19 shows that depending on the ligand L these compounds vary from Class III (fully delocalized Creutz−Taube ion) to strongly localized (compound **5** in ref 19, L = bis(4-pyridine) methane). For the compound in which the bridging pyrazine has been replaced by the 4,4′-bipyridyl ligand (compound **2** in ref 19), we obtain $\lambda = 4.02$, $\beta = 5$, and $\omega = 300$ cm^{-1},[24] and therefore this system can be placed on the boarder line between Classes I and II. It is worth mentioning that the degree of delocalization can be efficiently controlled by the length and conformation of the bridging ligands. In particular, the longer bridge can significantly reduce the electronic coupling and enhance the degree of localization.

At low temperatures and strong enough coupling, one can consider the tunneling splitting of the ground vibrational level $n = 0$. To simplify the evaluation of the tunneling splitting, one can apply the semiclassical Wentzel, Kramers, and Brillouin (WKB) approach that gives the following expression for the tunneling splitting gap δ in a double-well potential[34]

$$\delta = 2\hbar\tilde{\omega}\exp[-\int_b^c p(q)\mathrm{d}q] \tag{9}$$

In this expression, $\tilde{\omega}$ is the frequency of the oscillation at the bottom of the well that is in general different from ω; a and b are the classical turning points (Figure 3) for this oscillation; and $p(q)$ is the linear momentum conjugated with q

$$p(q) = \sqrt{2[U_-(q) - \varepsilon_0]/\hbar\omega} \tag{10}$$

dx.doi.org/10.1021/jp211057e | J. Phys. Chem. C 2012, 116, 4999−5008

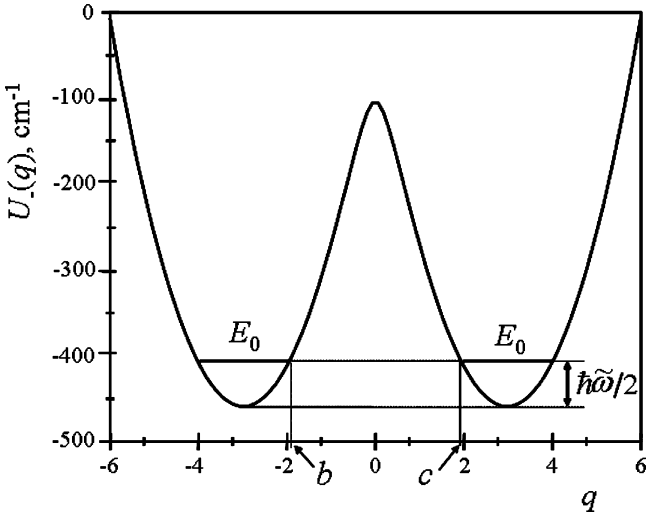

Figure 3. Illustration for the WKB approach: lower sheet of the adiabatic potential, ground vibrational level, and the classical turning points, $\lambda = 3$, $\beta = 1$, $\hbar\omega = 100$ cm^{-1}.

Here ε_0 is the energy of the degenerate level with $n = 0$ that is different from the energy $\varepsilon_A(n = 0) = \varepsilon_B(n = 0)$ of the ground vibrational level in eq 5 calculated with $\beta = 0$. One can see that the frequency of tunneling δ/h is the product of the doubled frequency $\tilde{\nu} = \tilde{\omega}/2\pi$ of the hits of the barrier wall and the exponential tunneling factor, which is the probability of tunneling through the barrier at each hit.

To calculate ε_0 and $\tilde{\omega}$, one has to expand the adiabatic potential $U_-(q)$ in the Taylor series near the minima. For example, expanding $U_-(q)$ near the left minimum and retaining the first two nonvanishing terms one obtains

$$U_-^{q<0}(q) \approx U_-(q_m^-) + \frac{1}{2}\left(\frac{d^2U_-}{dq^2}\right)_{q=\bar{q}_m}(q - q_m^-)^2 = -\frac{\hbar\omega}{2}\left(\lambda^2 + \frac{\beta^2}{\lambda^2}\right) + \frac{\hbar\omega}{2}\left(1 - \frac{\beta^2}{\lambda^4}\right)(q - q_m^-)^2 \quad (11)$$

The expression for $U_+^{q>0}(q)$ can be obtained by the substitution $q_m^- \rightarrow q_m^+$. Using this result we can define the following Hamiltonian of the vibrations near the left minimum

$$\hat{H}^{(q<0)} = -\frac{\hbar\omega}{2}\left(\lambda^2 + \frac{\beta^2}{\lambda^2}\right) + \frac{\hbar\omega}{2}\left(1 - \frac{\beta^2}{\lambda^4}\right)(q - q_m^-)^2 - \frac{\hbar\omega}{2}\frac{\partial^2}{\partial(q - q_m^-)^2} \quad (12)$$

Let us pass to the new coordinate $\tilde{q}_- = \gamma(q - q_m^-)$ and introduce the effective frequency $\tilde{\omega}$ such that the Hamiltonian takes on the oscillator form

$$\hat{H}^{(q<0)} = -\frac{\hbar\omega}{2}\left(\lambda^2 + \frac{\beta^2}{\lambda^2}\right) + \frac{\hbar\tilde{\omega}}{2}\left(\tilde{q}_-^2 - \frac{\partial^2}{\partial\tilde{q}_-^2}\right) = -\frac{\hbar\omega}{2}\left(\lambda^2 + \frac{\beta^2}{\lambda^2}\right) + \frac{\hbar\tilde{\omega}}{2}\gamma^2(q - q_m^-)^2 - \frac{\hbar\tilde{\omega}}{2\gamma^2}\frac{\partial^2}{\partial(q - q_m^-)^2} \quad (13)$$

By comparing eqs 12 and 13, one finds

$$\tilde{\omega}\gamma^2 = \omega\left(1 - \frac{\beta^2}{\lambda^4}\right), \quad \frac{\tilde{\omega}}{\gamma^2} = \omega \quad (14)$$

Solving this system of equations, one can find the renormalized frequency of the nuclear vibrations at the bottom of the lower sheet $U_-(q)$

$$\tilde{\omega} = \omega\sqrt{1 - \frac{\beta^2}{\lambda^4}}, \quad \gamma = \left(1 - \frac{\beta^2}{\lambda^4}\right)^{1/4} \quad (15)$$

One can see that the pseudo JT effect results in the "softening" of the system ($\tilde{\omega} < \omega$) which complies with the general principles of the pseudo JT effect.[27a,b] Then the eigenvalues of the Hamiltonian, eq 13, are the following

$$\varepsilon_n^{(q<0)} = -\frac{\hbar\omega}{2}\left(\lambda^2 + \frac{\beta^2}{\lambda^2}\right) + \hbar\tilde{\omega}\left(n + \frac{1}{2}\right) = -\frac{\hbar\omega}{2}\left(\lambda^2 + \frac{\beta^2}{\lambda^2}\right) + \hbar\omega\sqrt{1 - \frac{\beta^2}{\lambda^4}}\left(n + \frac{1}{2}\right) \quad (16)$$

and the same expression is evidently true for $\varepsilon_n^{(q>0)}$. Therefore the energy of the ground double degenerate level is given by

$$\varepsilon_0 = \frac{\hbar\omega}{2}\left(\sqrt{1 - \frac{\beta^2}{\lambda^4}} - \lambda^2 - \frac{\beta^2}{\lambda^2}\right) \quad (17)$$

Finally, the classical turning points are found by solving the equation $U_-(q) = \varepsilon_0$, and therefore within the WKB approach, eq 9, one obtains the splitting δ as function of λ, β, and $\hbar\omega$. Thus, for the Ru^{II}/Ru^{III} compound with L = bipyridyl, we find $\delta = 0.4 \times 10^{-3}$ cm^{-1}. For the more strongly coupled $[\{Ru(NH_3)_5\}_2(\mu\text{-}Cl_4dicyd^{2-})]^{3+}$ complex (but still belonging to Class IIA according to ref 18), this value is expected to be much larger. In this case however the WKB approach is probably a poor approximation so that a reliable estimation of δ requires a numerical solution of the dynamic vibronic pseudo JT problem that will not be considered in the present study. In the modeling of the LZ transitions, we will use in our sample calculations the following two sets of parameters that fall in a reasonable range for Class IIA compounds

(i) $\lambda = 3$, $\beta = 1$, $\hbar\omega = 100$ cm^{-1}.
With these parameters, one obtains the following values:

$$b \approx -1.975,\ c \approx 1.975,\ \tilde{\omega} \approx 0.994\omega,\ \varepsilon_0 = -405.865\ \text{cm}^{-1},\ \delta \approx 0.353\ \text{cm}^{-1}$$

(ii) $\lambda = 3$, $\beta = 0.5$, $\hbar\omega = 100$ cm^{-1}.
In this case, one obtains:

$$b = -1.994,\quad c = 1.994,\quad \tilde{\omega} \approx 0.998\omega,\ \varepsilon_0 = -401.466\ \text{cm}^{-1},\quad \delta \approx 0.27\ \text{cm}^{-1}$$

These two cases show how the tunneling splitting increases with the increase of the parameter β and/or with the decrease of λ.

dx.doi.org/10.1021/jp211057e | J. Phys. Chem. C 2012, 116, 4999−5008

3. EFFECTS OF THE TIME-DEPENDENT ELECTRIC FIELD AND LANDAU–ZENER TUNNELING IN A ONE-ELECTRON MIXED VALENCE DIMER

Let us first consider the MV dimer in an external static electric field that is directed along the Z-axis. The Hamiltonian of the interaction of a MV dimer with the electric field is the following

$$\hat{H}_d = -\hat{d}_Z E_Z \tag{18}$$

where $\hat{d}_Z$ is the electric dipole moment operator defined by the following matrix

$$\hat{d}_Z = \begin{array}{c} \\ \varphi_A \\ \varphi_B \end{array} \begin{array}{c} \begin{array}{cc} \varphi_A & \varphi_B \end{array} \\ \begin{pmatrix} d_0 & 0 \\ 0 & -d_0 \end{pmatrix} \end{array}, \tag{19}$$

where $d_0 = eR/2$ and $\mathbf{R} \equiv \mathbf{R}_{AB}$. In the presence of the electric field, the effective two-level Hamiltonian involving only the two low-lying vibrational levels with $n = 0$ is represented by the following 2×2 matrix

$$\hat{H}_{eff} = \begin{array}{c} \\ \chi_0^A \\ \chi_0^B \end{array} \begin{array}{c} \begin{array}{cc} \chi_0^A & \chi_0^B \end{array} \\ \begin{pmatrix} \varepsilon_0 - d_0 E_Z & \delta/2 \\ \delta/2 & \varepsilon_0 + d_0 E_Z \end{pmatrix} \end{array}, \tag{20}$$

which is defined in the basis of the localized electron-vibrational states

$$\chi_0^A = \varphi_A \Phi_n(\tilde{q}_-) = \varphi_A \Phi_n[\gamma(q - q_m^-)],$$
$$\chi_0^B = \varphi_A \Phi_n(\tilde{q}_+) = \varphi_B \Phi_n[\gamma(q - q_m^+)] \tag{21}$$

Using the eigenvalues of this matrix, one obtains the following expressions for the electronic densities on the sites A and B

$$\rho_A = \frac{1}{2}\left[1 + \frac{d_0 E_Z}{\sqrt{\delta^2 + (d_0 E_Z)^2}}\right],$$
$$\rho_B = \frac{1}{2}\left[1 - \frac{d_0 E_Z}{\sqrt{\delta^2 + (d_0 E_Z)^2}}\right] \tag{22}$$

One can see that the electric field of the chosen direction decreases the electronic density on the site B and increases it on the site A, thus producing a trapping effect which increases with the decrease of the tunneling splitting δ as shown in Figure 4. The tunneling splitting δ is assumed to be relatively small in the sense that the electric field that can be achieved under the real experimental condition would be able to significantly localize the system.

Let us consider the effect of a short electric pulse of the Gaussian form that acts on the system along with a static field. The total field including both time-independent and time-dependent contributions can be defined as follows

$$E_Z(t) = E_0 - pE_0 \exp\left(-\frac{t^2}{2\tau^2}\right) \tag{23}$$

where τ is the characteristic time of the pulse. Time dependences of the applied electric field are illustrated in Figure 5 (upper part).

In the presence of the time-dependent electric field, the effective two-level Hamiltonian takes on the following form

$$\hat{H}_{eff} = \begin{array}{c} \\ \chi_0^A \\ \chi_0^B \end{array} \begin{array}{c} \begin{array}{cc} \chi_0^A & \chi_0^B \end{array} \\ \begin{pmatrix} \Delta/2 & \delta/2 \\ \delta/2 & -\Delta/2 \end{pmatrix} \end{array}, \tag{24}$$

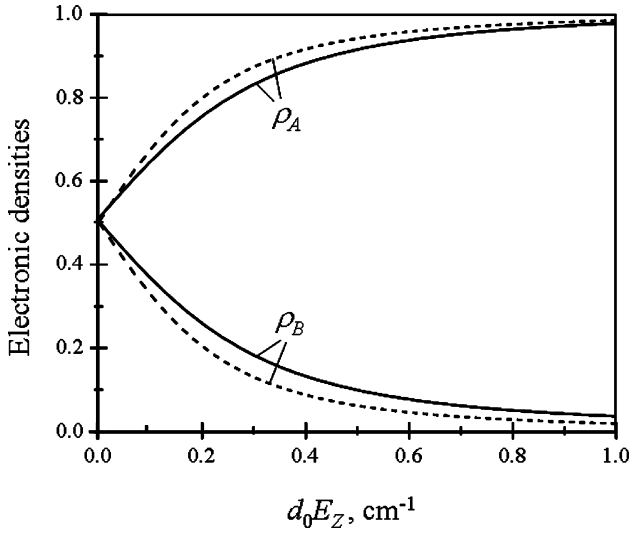

Figure 4. Electronic densities on the sites A and B calculated as functions of d_0E_Z at δ = 0.353 cm^{-1} (solid lines) and δ = 0.27 cm^{-1} (dashed lines).

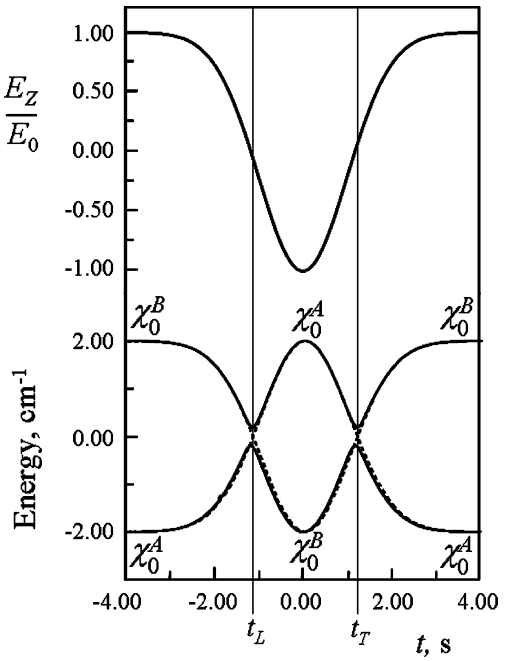

Figure 5. Time dependence of the applied electric field for a Gaussian pulse (upper part) and time dependence of the adiabatic (solid lines) and diabatic (dashed lines) levels (lower part): τ = 1 s, d_0E_0 = 2 cm^{-1}, δ = 0.353 cm^{-1}, p = 2.

In eq 24 the value

$$\Delta = -2d_0E_0\left[1 - p\exp\left(\frac{t^2}{2\tau^2}\right)\right] \tag{25}$$

is the energy gap between the diabatic (δ = 0) levels. The diabatic levels crossing (Δ = 0) occurs at times $t_T = -t_L = \tau(2\ln(p))^{1/2}$, where the times t_T and t_L relate to the trailing (T) and the leading (L) edges of the pulse, respectively (Figure 5,

dx.doi.org/10.1021/jp211057e | J. Phys. Chem. C 2012, 116, 4999–5008

upper part). Then one can find the following adiabatic time-dependent energies (Figure 5, low part)

$$\varepsilon_{\pm} = \pm\frac{1}{2}\sqrt{\Delta^2 + \delta^2} = \pm\sqrt{(d_0E_0)^2[1 - p\exp(-t^2/2\tau^2)]^2 + \delta^2/4} \quad (26)$$

They pass through the anticrossing points at times $t = t_L$ and $t = t_T$ for which the diabatic levels cross. After the anticrossing point, the system changes the site of localization and consequently the direction of polarization. The adiabatic approximation breaks down in the vicinity of these two anticrossing areas, and the system undergoes intensive transitions between the ground and excited states via the LZ mechanism[13] that has been intensively employed in the study of SMMs.[1] One can see that the LZ transitions in the system under study can be observed providing $p > 1$.

The key parameter that is the time-dependent sweep rate of the applied electric field $c(t) = d\Delta/dt$ is calculated as follows

$$c(t) = -\frac{2pd_0E_0t}{\tau^2}\exp\left(-\frac{t^2}{2\tau^2}\right) \quad (27)$$

At the crossing points, the sweep rate takes the values

$$c(t_L) = -c(t_T) \equiv c = \frac{2d_0E_0}{\tau}\sqrt{2\ln(p)} \quad (28)$$

Using the fact that the time interval for the LZ transitions is narrow (comparatively to the pulse duration), one can assume the linear time dependence of the gap between the diabatic levels near the crossing points. One can thus expand the function $\Delta(t)$ in the Taylor series near the points t_L and t_T and retain only linear terms of this expansion, that is

$$\Delta(t) = c(t_L)(t - t_L) \text{ near } t_L;$$

$$\Delta(t) = c(t_T)(t - t_T) \text{ near } t_T$$

In the present consideration, we assume that the tunneling is coherent (see ref 35). In principle, the coherence is affected by the interaction of the molecular system with the thermal bath and by the dipole−dipole interactions. These complicated factors are worthy to be specially studied. Nevertheless, one can mention the experimental data that unambiguously argue in favor of the cases for which the decoherence in MV systems can be regarded as weak. In fact, recent observation of the Rabi oscillations in MV systems and the subsequent analysis of the coherent states (see ref 32 and refs therein) evidence in favor of applicability of the model based on the LZ theory dealing with the coherent tunneling at each passage. It should be mentioned also that the tunneling splitting δ in MV systems is several orders larger than in SMMs, so the pulse in the former case should be shorter, and consequently the condition of coherency can be satisfied. This seems to be valid even if one takes into account that the electron phonon interaction and electric dipole−dipole interactions in MV systems are stronger than the spin−phonon and magnetic dipole−dipole interactions in SMMs. The question of coherency in MV systems requires special consideration that is beyond the present paper. For the sake of simplicity, we assume also that although each LZ passage is coherent the time between two passages is long enough to average the Stückelberg phase that will be ruled out from the present consideration.

For the coherent tunneling, the classical LZ formula can be used for the probability of the transition between the ground and excited states at the leading edge of the pulse[13]

$$P = \exp[-\pi\delta^2/(2\hbar c)] \quad (29)$$

The LZ tunneling at the leading edge of the pulse is schematically illustrated in Figure 6, where the diabatic and adiabatic levels are plotted as functions of Δ near the point $\Delta(t_L) = 0$. It is seen that the transition from the ground state to the excited one is not accompanied by the change of the localization site of the extra electron, and therefore P is the probability for the system to retain the A-localization of the extra electron, that is, $P = P^L_A$. On the contrary, if the system remains in the ground state, the extra electron changes its localization, and the probability of this event is $P^L_{A\to B} = 1 - P$.

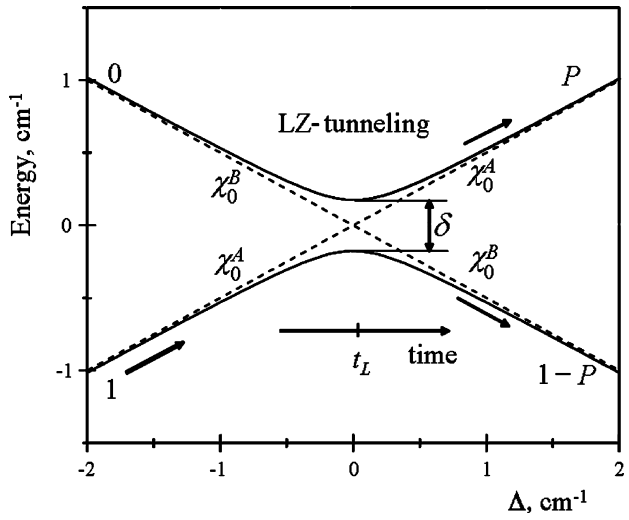

Figure 6. Illustration for the LZ tunneling at the leading edge of the pulse: diabatic (dashed lines) and adiabatic (solid lines) levels calculated with $\delta = 0.353$ cm^{-1} are plotted as functions of Δ near the point $\Delta(t_L) = 0$.

In the adiabatic limit ($c \to 0$), the change of the localization is complete, i.e., $P = 0$, $P^L_{A\to B} = 1$ (flip of the dipole moment), and for very fast sweeps ($c \to \infty$), the system passes to the exited state retaining the site of localization A ($P = 1$, $P^L_{A\to B} = 0$). Finally, for the intermediate values of the sweep rate ($0 < P < 1$, $0 < P^L_{A\to B} < 1$), the change of the localization is partial. Since the pulse of the electric field is symmetric, the transition probability $P^T_i(i = A,B)$ at the trailing edge of the pulse ($t \sim t_T$) coincides with the probability P^L_i at the leading edge of the pulse ($t \sim t_L$), that is, $P^T_i = P^L_i = P$.

To evaluate the distribution of the probabilities after the pulse, i.e., probabilities induced by the two successive LZ transitions, the following arguments related to the kinetics can be employed. The probabilities P, or alternatively populations per molecule (initial polarization), and $1 - P$ (reversed polarization) resulted from the first passage at the leading edge of the pulse can be considered as initial ones with respect to the passage through the second anticrossing point (at the trailing edge) (Figure 5). Let us denote the populations (per molecule) before the pulse as $n_A(t < t_L)$ and $n_B(t < t_L)$ (that are assumed to be 1 and 0). These values after the first passage will be $n_A(t_L < t < t_T) = P$ and $n_B(t_L < t < t_T) = 1 - P$, and finally after the pulse they become $n_A(t > t_T)$, $n_B(t > t_T)$ where the order of the

dx.doi.org/10.1021/jp211057e | J. Phys. Chem. C 2012, 116, 4999−5008

levels subjected to two anticrossing points can be identified from Figure 5. Then one can write down

$$n_A(t > t_T) = n_B(t_L < t < t_T)(1 - P) + n_A(t_L < t < t_T)P = 1 - 2P(1 - P)$$

$$n_B(t > t_T) = n_A(t_L < t < t_T)(1 - P) + n_B(t_L < t < t_T)P = 2P(1 - P) \quad (30)$$

One can see that the total probability for the system pass in the excited (to change polarization) will be $P_{A\to B} = 2P(1 - P)$, while the probability to remain in the ground state after the pulse (conventionally, $t \gg t_T$), i.e., to retain the site of localization, is $P_A = 1 - 2P(1 - P)$. For the Gaussian pulse so far considered one finds

$$P_{A\to B} = 2\exp\left[-\frac{\pi\delta^2\tau}{4\hbar d_0 E_0\sqrt{2\ln(p)}}\right] \times \left\{1 - \exp\left[-\frac{\pi\delta^2\tau}{4\hbar d_0 E_0\sqrt{2\ln(p)}}\right]\right\} \quad (31)$$

If the time-dependent wave function $\psi(t)$ was initially $\psi(t \ll t_L) = \chi_0^A$, then at times $t \gg t_T$, it becomes the following superposition

$$\psi(t \gg t_T) = c_A\chi_0^A + c_B\chi_0^B \quad (32)$$

where

$$|c_A|^2 = P_A, \quad |c_B|^2 = P_{A\to B} \quad (33)$$

The probabilities to conserve the localization of the extra electron (P_A) and to change it ($P_{A\to B}$) as functions of τ are shown in Figure 7. It is seen that $P_{A\to B}$ is close to 0, and P_A is close to 1 for short and long pulses. At the time point

$$\tau_m = 4\ln(2)\hbar d_0 E_0(\pi^{-1}\delta^{-2})\sqrt{2\ln(p)} \quad (34)$$

the curve $P_{A\to B}(\tau)$ reaches its maximum, and $P_A(\tau)$ becomes minimal with $(P_{A\to B})_{max} = (P_A)_{min} = 1/2$. This means that at $\tau = \tau_m$ in half of MV dimers the extra electron changes the site of localization giving rise to a flip of their electric dipole moments, while for all other values of τ the number of such dimers is less than half of their total number.

As follows from eq 34, the duration of the pulse leading to efficient LZ transitions must be reduced when one passes to the systems with larger tunneling splitting. Simultaneously for larger δ, the field E_0 must be stronger to be able to suppress the tunneling. The dependence of τ_m upon E_0 is however less pronounced than the dependence upon δ. Thus, if one passes from $\delta = 0.353$ cm^{-1} to $\delta = 20$ cm^{-1} and increases d_0E_0 from 2 to 100 cm^{-1} to ensure strong localizion before the pulse, one finds that the pulse time τ_m becomes almost two orders shorter (1.38×10^{-12} s instead of 8.86×10^{-11} s). One can see that even for a relatively large tunneling we obtain feasible values of the constant electric field and for the duration of the pulse (picosecond laser pulses). The shorter pulses (shorter than the decoherence time) provide better conditions for the observation of coherent tunneling. In principle, the study of even larger tunneling splitting seems to be feasible with the use of the femtosecond laser pulses.

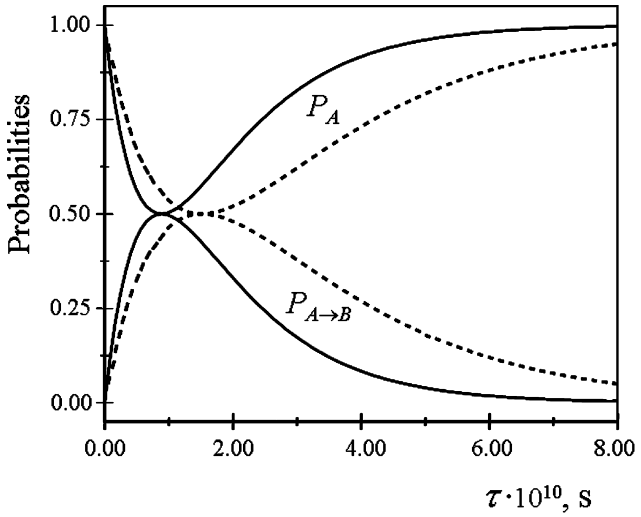

Figure 7. Probabilities $P_{A\to B}$ and P_A as functions of τ calculated with $d_0E_0 = 2$ cm^{-1} and $p = 2$ for the d^1–d^0 dimer with $\delta = 0.353$ cm^{-1} (solid lines) and $\delta = 0.27$ cm^{-1} (dashed lines). Alternatively, these curves show $P^S_{A\to B}(\tau)$ and $P^S_A(\tau)$ functions calculated at $\beta = 1$, $\lambda = 3$, and $\hbar\omega = 100$ cm^{-1} for $S = 3/2$ (solid lines) and $S = 1/2$ (dashed lines) states of a d^2–d^1 dimer.

An alternative way to characterize the nonadiabatic LZ transition is to plot the change of the expectation value of the electric dipole moment as a function of τ. We thus obtain that $\bar{d}_Z$ after the pulse is given by

$$\bar{d}_Z(t \gg t_T) = P_A d_0 - P_{A\to B}d_0 = d_0(1 - 2P_{A\to B}) \quad (35)$$

On the other hand, the initial (before the pulse) $\bar{d}_Z$ value is

$$\bar{d}_Z(t \ll t_L) = d_0 \quad (36)$$

Then the LZ transition will be characterized by the parameter

$$r = \frac{\bar{d}_Z(t \ll t_L) - \bar{d}_Z(t \gg t_T)}{d_0} = 2P_{A\to B} \quad (37)$$

that is the dimensionless change of the dipole moment under the action of the electric pulse. From the plot of this value as a function of τ (Figure 8), one can see that $r \to 0$ (no flipping of the electric dipole moments) providing $\tau \to 0$ or $\tau \to \infty$. On the other hand, at $\tau = \tau_m$ one finds that $\bar{d}_Z(t \gg t_T) = 0$ (the initial electric polarization is fully destroyed by the pulse), and the function $r(\tau)$ reaches its maximum value $r_{max} = 1$ at $\tau = \tau_m$.

4. EFFECT OF THE DOUBLE EXCHANGE ON THE LANDAU–ZENER TRANSITIONS

In a more general case, the itinerant electron travels over localized spins (the so-called spin cores), and the double exchange coupling becomes operative. The interaction of the localized and delocalized spins through the double exchange[29] results in the ferromagnetic effect in MV systems (with the exception of special cases of frustration[16,36]). The transfer integral becomes spin-dependent (it will be denoted as β_S) as it was discovered for the double exchange mechanism with the spin dependence being the following

$$\beta_S = \frac{\beta(S + 1/2)}{(2s_0 + 1)} \quad (38)$$

where S is the total spin of the dimer, and s_0 is the spin of the spin core.

dx.doi.org/10.1021/jp211057e | J. Phys. Chem. C 2012, 116, 4999–5008

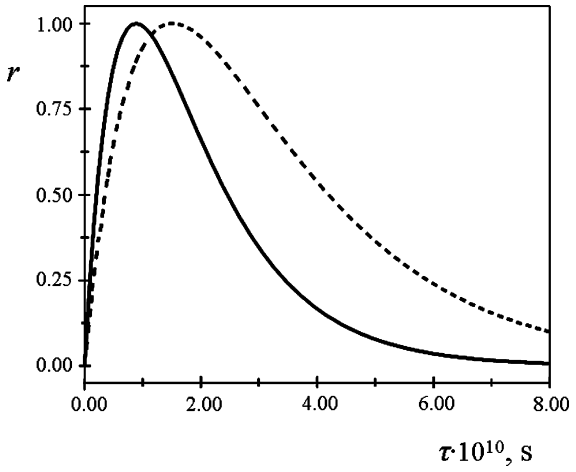

Figure 8. Values r vs τ plot calculated with $d_0E_0 = 2$ cm^{-1} and $p = 2$ for the d^1–d^0 dimer with $\delta = 0.353$ cm^{-1} (solid line) and $\delta = 0.27$ cm^{-1} (dashed line). Alternatively, these curves show r^S vs τ plots calculated with $\beta = 1$, $\lambda = 3$, and $\hbar\omega = 100$ cm^{-1} for $S = 3/2$ (solid) and $S = 1/2$ (dotted) states of the d^2–d^1 dimer.

In the simplest case of the many-electron MV dimer of d^2–d^1-type, the spin cores $s_0 = 1/2$, and the total spin takes on the values $S = 1/2$, $3/2$, and $\beta_{1/2} = \beta/2$, $\beta_{3/2} = \beta$. As a result, the tunneling splitting δ proves to be also spin-dependent. Denoting this splitting as δ_S and keeping in mind that the vibronic parameter λ is independent of S, one arrives at the conclusion that $\delta_{3/2} > \delta_{1/2}$. Particularly, for $\beta = 1$ one finds $\beta_{1/2} = 0.5$ and $\beta_{3/2} = 1$, and the parameters $\delta_{3/2}$ and $\delta_{1/2}$ for this case have already been calculated: $\delta_{3/2} \approx 0.353$ cm^{-1} and $\delta_{1/2} \approx 0.27$ cm^{-1}.

The probabilities $P_{A\to B}$ and P_A and the response r proves to be also spin-dependent as shown in Figures 7 and 8. Thus, the curves shown by solid lines describe the LZ transitions for the state with $S = 3/2$, and those shown by dotted lines relate to the state with $S = 1/2$. It follows from eq 34 that $\tau_m \sim \delta^{-2}$, so the position of the extremum in the $P^S_{A\to B}(\tau)$, $P^S_A(\tau)$, and $r^S(\tau)$ dependences is shifted to the area of smaller τ when we pass from the state with $S = 1/2$ to the state with $S = 3/2$.

Along with the double exchange, the Heisenberg–Dirac–Van–Vleck (HDVV) exchange interaction is also operative in the many-electron MV clusters. This interaction acts within each electron localization and is defined by the spin Hamiltonian

$$H_{ex} = -2Js_As_B \tag{39}$$

where J is the exchange parameter. The combined action of the double exchange and HDVV exchange leads to the following spin-dependent diabatic energies ε_0^S at $E_Z = 0$

$$\varepsilon_0^{S=1/2} = 2J + \frac{\hbar\omega}{2}\left(\sqrt{1 - \frac{\beta^2}{4\lambda^4}} - \lambda^2 - \frac{\beta^2}{4\lambda^2}\right),$$

$$\varepsilon_0^{S=3/2} = -J + \frac{\hbar\omega}{2}\left(\sqrt{1 - \frac{\beta^2}{\lambda^4}} - \lambda^2 - \frac{\beta^2}{\lambda^2}\right) \tag{40}$$

In most cases of transition metal complexes, the exchange interaction is antiferromagnetic ($J < 0$) tending thus to stabilize the energy level with $S = 1/2$ with respect to that with $S = 3/2$.

For example, in the case of relatively weak exchange interaction ($J = -2$ cm^{-1}) and providing $\lambda = 3$, $\beta = 1$, and $\hbar\omega = 100$ cm^{-1}, one obtains the following values of energies ε_0^S at $E_Z = 0$

$$\varepsilon_0^{S=1/2} = -405.466 \text{ cm}^{-1},\ \varepsilon_0^{S=3/2} = -403.865 \text{ cm}^{-1}$$

One can see that in the ground diabatic level at $E_Z = 0$ the system possesses the lowest full spin $S = 1/2$. The same is true when $E_Z \neq 0$, and hence in the low-temperature limit when the excited levels are not populated only the $S = 1/2$ component is affected by the pulse of the electric field and participates in the LZ transitions. The LZ tunneling regime can be, however, changed by applying the static magnetic field. In fact, if this field is strong enough, the states with $S = 3/2$ can become active in the LZ transitions as illustrated in Figure 9.

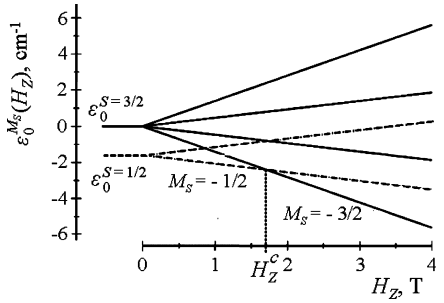

Figure 9. Diabatic levels of the d^2–d^1 system in the applied static magnetic field, $J = -2$ cm^{-1}, $\lambda = 3$, $\beta = 1$, and $\hbar\omega = 100$ cm^{-1}. The level $\varepsilon_0^{S=3/2}$ at $H_Z = 0$ is chosen as a reference point.

When the magnetic field is smaller than the critical value H_Z^c that is the crossing point (≈1.714 T for the chosen set of parameters)

$$H_Z^c = \frac{1}{g_e\mu_B}\left[-3J + \frac{\hbar\omega}{2}\left(-\frac{3\beta^2}{4\lambda^2} + \sqrt{1 - \frac{\beta^2}{\lambda^4}} - \sqrt{1 - \frac{\beta^2}{4\lambda^4}}\right)\right] \tag{41}$$

the Zeeman sublevel with $M_S = -1/2$ arising from the $S = 1/2$ multiplet is the ground state, while at $H_Z > H_Z^c$ the sublevel $S = 3/2$, $M_S = -3/2$ becomes the ground state. Since the electron transfer does not change the total spin projection of the dimer, the LZ shows the change of the adiabatic levels of the d^2–d^1 dimer under the action of the static magnetic field. In the absence of the magnetic field, the ground adiabatic level possesses the spin $S = 1/2$ (Figure 10a), and this is the only state participating in the LZ transition with the response $r^{1/2}$. At the applied field $H_Z = 3T > H_Z^c$ (Figure 10b) the adiabatic level with $M_S = 3/2$ arising from the state with $S = 3/2$ becomes the ground state, and the electric response to the electric field pulse is $r^{3/2}$. The change of the responses $\Delta r = r^{M_S=3/2} - r^{M_S=1/2}$ while passing from the $H_Z < H_Z^c$ to $H_Z > H_Z^c$ regime nonmonotonically depends on the time of the pulse τ as shown in Figure 11. At short pulses, $r^{M_S=3/2}$ exceeds $r^{M_S=1/2}$, while for long pulses one obtains that $r^{M_S=3/2} < r^{M_S=1/2}$.

Therefore, we arrive at the conclusion that electric polarization in MV systems induced by the electric pulse and magnetization of the system due to the double exchange and HDVV exchange are interrelated in the presence of the external magnetic field. The total dipole moment of the many-electron

dx.doi.org/10.1021/jp211057e | J. Phys. Chem. C 2012, 116, 4999–5008

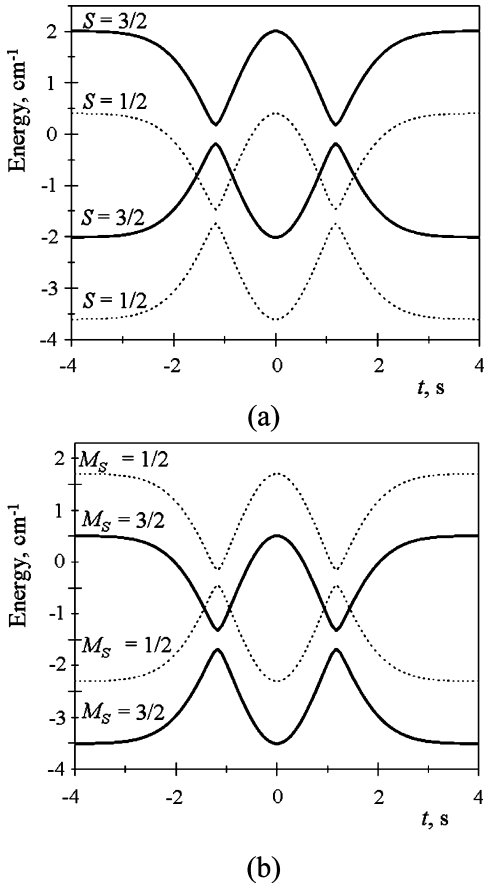

Figure 10. Time dependence of the adiabatic levels of d^2–d^1 dimer calculated with $J = -2$ cm^{-1}, $\lambda = 3$, $\beta = 1$, and $\hbar\omega = 100$ cm^{-1} at $H_Z = 0$ (a) and at $H_Z = 3$ T (b). The levels with $S = 3/2$ and $S = 1/2$ are shown by solid and dotted lines, respectively. The anticrossing point for the levels with $S = 3/2$ is chosen as a reference point.

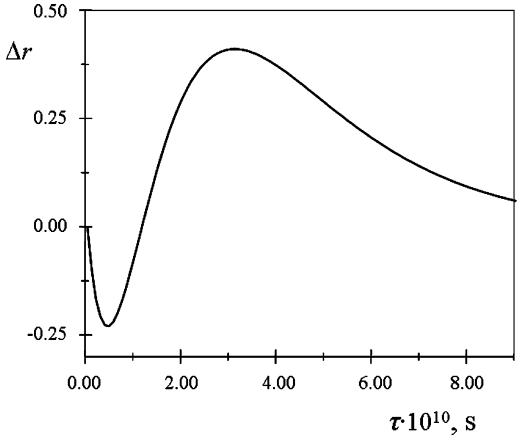

Figure 11. Change of the responses $\Delta r = r^{M_S=3/2} - r^{M_S=1/2}$ when passing from $H_Z < H_Z^c$ to $H_Z > H_Z^c$ as a function of τ.

MV systems can be controlled by both the electric field pulse and static magnetic field.

5. CONCLUDING REMARKS

In this article, we have proposed and theoretically studied a new scheme of the coherent LZ transitions triggered by an electric pulse in MV systems. These systems possess a large intrinsic electronic dipole moment that is suppressed by the tunneling between the potential wells separating the vibronically localized configuration. In this sense, a MV dimer can be conventionally referred to as single molecule ferroelectric by analogy with a single molecule magnet possessing an internal magnetic moment. Under certain conditions, a long-living dipole moment can be easily stabilized by an external electric field and efficiently controlled by an electric field pulse via the LZ transitions that in this paper are assumed to be coherent. The frames of the controllable properties of the MV systems are provided by employing the double exchange and the HDVV exchange in many-electron clusters in which the external magnetic field can be involved into the game.

To summarize, the following more specific issues should be mentioned:

1. The electric field pulse has been shown to induce the LZ transitions in MV clusters belonging to the Robin and Day Class II. It is shown that the probability to change the site of the localization of the excess electron and thus to reverse the electric dipole moment upon the action of the pulse ($t \gg t_T$) increases with the increase of the time τ of the pulse, reaches the maximal value 1/2, and then decreases. On the contrary, the probability to conserve the localization position is decreased when τ is increased, reaches the minimum that is equal to 1/2 (half of dimers are overturned), and then is increased to 1 (no reversal of the electric dipole moment) at long pulses. This provides a possible way to create controllable superposition of the states with different electron localizations that can be regarded as a proposal for the realization of qubits based on MV dimers.
2. An important peculiarity of the LZ tunneling in many-electron MV dimers in which the double exchange and HDVV exchange are operative is the spin-dependent character of the phenomenon. This opens a way to control the electric polarization of the system induced by the time-dependent electric field by applying an additional static magnetic field, which can stabilize different spin states. Such a possibility is of potential importance for applications of these systems as molecular electronic devices.
3. To our knowledge, the direct observation of the tunneling splitting of the low-lying vibrational levels in MV clusters has not been performed until now. On the other hand, the intervalence transfer bands, which have been extensively discussed in the literature, provide only indirect information about the tunneling splitting (mainly the reorganization energy and the value of the electron transfer matrix element). In this paper, we have suggested to employ the electric field pulse as a tool for the direct observation of the tunneling splitting through the coherent LZ transitions.
4. The theory reported here can be regarded as a first step in the study of the nonadiabatic LZ tunneling in MV compounds. It is applicable only in the low-temperature limit and neglects the decoherence effects arising from the electric dipole–dipole interactions between MV dimers and from the interactions of the electric dipoles with phonons. Although the assumption of the coherent tunneling in some cases can be realistic (as it was argued by the observation of the Rabi oscillations in MV systems), the development of a more comprehensive theory of incoherent LZ tunneling in MV clusters accompanied by the

dx.doi.org/10.1021/jp211057e | J. Phys. Chem. C 2012, 116, 4999–5008

experimental study of the LZ transitions seems to be the next step toward the better understanding of this fascinating phenomenon and its possible applications in the design of nanoelectronic devices.

AUTHOR INFORMATION

Corresponding Author

*E-mail: andrew.palii@uv.es (A.P.); tsuker@bgu.ac.il (B.T.).

Notes

The authors declare no competing financial interest.

ACKNOWLEDGMENTS

A.P. gratefully acknowledges the University of Valencia for visiting research grant, financial support from STCU (project N 5062), and the Supreme Council on Science and Technological Development of Moldova. B.T. thanks the Israel Science Foundation (ISF) for the financial support (grant no. 168/09). J.M.C.J. and E.C. thank Spanish MICINN (CSD2007-00010 CONSOLIDER-INGENIO in Molecular Nanoscience, MAT2007-61584, CTQ-2008-06720 and CTQ-2005-09385), Generalitat Valenciana (PROMETEO program), and the EU (ELFOS project and ERC Advanced Grant SPINMOL) for financial support.

REFERENCES

(1) Gatteschi, D.; Sessoli, R. ; Villain, J. *Molecular Nanomagnets*; Oxford University Press: Oxford, 2006. (b) Gatteschi, D.; Sessoli, R. *Angew. Chem., Int. Ed.* **2003**, *42*, 268−297.

(2) Friedman, J. R.; Sarachik, M. P.; Tejada, J.; Ziolo, R. *Phys. Rev. Lett.* **1996**, *76*, 3830−3833.

(3) Miller, J. S.; Epstein, A. J. *MRS Bull.* **2000**, *25*, 21−30.

(4) (a) Wernsdorfer, W.; Sessoli, R. *Science* **1999**, *284*, 133−135. (b) Wernsdorfer, W.; Ganneschi, A.; Sessoli, R.; Gatteschi, D.; Cornia, A.; Villar, V.; Pulsen, C. *Phys. Rev. Lett.* **2000**, *84*, 2965−2968.

(5) Christou, G.; Gatteschi, D.; Hendrickson, D. N.; Sessoli, R. *MRS Bull.* **2000**, *25*, 66−71.

(6) Sessoli, R.; Tsai, H.-L.; Schake, A. R.; Wang, S. J.; Vincent, B.; Folting, K.; Gatteschi, D.; Christou, G.; Hendrickson, D. N. *J. Am. Chem. Soc.* **1993**, *115*, 1804−1816.

(7) (a) Miyashita, S. J. *Phys. Soc. Jpn.* **1995**, *64*, 3207−3214. (b) Miyashita, S. *J. Phys. Soc. Jpn.* **1996**, *65*, 2734−2735.

(8) Dobrovitski, V. V.; Zvezdin, A. K. *Europhys. Lett.* **1997**, *38*, 377−382.

(9) Gunther, L. *Europhys. Lett.* **1997**, *39*, 1−6.

(10) De Raedt, H.; Miyashita, S.; Saito, K.; García-Pablos, D.; García, N. *Phys. Rev. B* **1997**, *56*, 11761−11768.

(11) Wernsdorfer, W.; Sessoli, R.; Caneschi, A.; Gatteschi, D.; Cornia, A. *Europhys. Lett.* **2000**, *50*, 552−558.

(12) Leuenberger, M. N.; Loss, D. *Phys. Rev. B* **2000**, *61*, 12200−12203.

(13) (a) Landau, L. *Phys. Z. Sowjetunion* **1932**, *2*, 46. (b) Zener, C. *Proc. R. Soc. London, Ser. A* **1932**, *137*, 696−702. (c) Stückelberg, E. C. G. *Helv. Phys. Acta* **1932**, *5*, 369−422.

(14) Day, P; Hush, N. S.; Clark, R. J. H. *Phil. Trans. R. Soc. A* **2008**, *366*, 5−14.

(15) (a) Robin, M. B.; Day, P. *Adv. Inorg. Chem. Radiochem.* **1967**, *10*, 247−422. (b) Hush, N. S. *Prog. Inorg. Chem.* **1967**, *8*, 391−444. (c) Piepho, S. B.; Krausz, E. R.; Schatz, N. *J. Am. Chem. Soc.* **1978**, *100*, 2996−3005.

(16) (a) Borras-Almenar, J. J.; Clemente-Juan, J. M.; Coronado, E.; Palii, A. V.; Tsukerblat, B. Magnetic Properties of Mixed-Valence Systems: Theoretical Approaches and Applications. *Magnetoscience: From Molecules to Materials*; Miller, J., Drillon, M., Eds.; Wiley-VCH: New York, 2001; pp 155−210. (b) Tsukerblat, B; Klokishner, S.; Palii, A. Jahn-Teller Effect in Molecular Magnetism: An Overview. In: *The Jahn-Teller Effect. Fundamentals and Implications for Physics and Chemistry*; Springer Series in Chemical Physics; Springer, Heidelberg, Dordrecht: London, New York; Köppel, H., Yarkony, D. R., Barentzen, H., Eds.; 2009; Vol. *97*, Part V, pp 555−620.

(17) Solomon, E; Xie, X.; Dey, A. *Chem. Soc. Rev.* **2008**, *37*, 623−638.

(18) Brunschwig, B. S.; Creutz, C.; Sutin, N. *Chem. Soc. Rev.* **2002**, *32*, 168−184.

(19) Ward, M. *Chem. Soc. Rev.* **1995**, *34*, 121−134.

(20) (a) Reimers, J. R.; Hush, N. S. Electric Field Perturbation of Electronic (Vibronic) Absorption Envelopes: Application to Characterization of Mixed Valence States. In *Proceedings of the NATO Advanced Workshop on Mixed Valency Compounds: applications in Chemistry, Physics and Biology*; Series C, Prassides, K., Ed.; Kluwer Academic Publishers: Dordrecht, The Netherlands, 1990; Vol. *343*, pp 29−50. (b) Oh, D. H.; Boxer, S. G. *J. Am. Chem. Soc.* **1990**, *112*, 8161−8162.

(21) Brunschwig, B. S.; Creutz, C.; Sutin, N. *Coord. Chem. Rev.* **1998**, *177*, 61−79.

(22) Treynor, T. P.; Boxer, S. G. *J. Phys. Chem. A* **2004**, *108*, 1764−1778.

(23) Kanchanawong, P; Dahlbom, M. G.; Treynor, T. P.; Reimers, J. R.; Hush, N. S.; Boxer, S. G. *J. Phys. Chem. B* **2006**, *110*, 18688−18702.

(24) Silverman, L. N.; Kanchanawong, P.; Treynor, T. P.; Boxer, S. G. *Phil. Trans. R. Soc. A* **2008**, *366*, 33−45.

(25) Leggett, A. I.; Chakravarty, S.; Dorsey, A. T.; Fisher, M. P. A.; Garg, A.; Zwerger, W. *Rev. Mod. Phys.* **1987**, *59*, 1−85.

(26) Cukier, R. I.; Morillo, M. In *Molecular Electronics*; Jortner, J., Ratner, M., Eds.; Blackwell Science: Cambridge, MA, 1997; pp 119−156.

(27) (a) Bersuker, I. B.; Polinger, V. Z. *Vibronic Interactions in Molecules and Crystals*; Springer-Verlag: New York, 1989. (b) Bersuker, I. B. *The Jahn-Teller effect*; University Press: Cambridge, 2006. (c) Bersuker, I. B.; Borshch, S. A. *Adv. Chem. Phys.* **1992**, *81*, 703−782.

(28) Palii, A.; Tsukerblat, B.; Clemente-Juan, J. M.; Gaita-Ariño, A. *Phys. Rev. B* **2011**, *84*, 184426-1−184426-11.

(29) (a) Zener, C. *Phys. Rev.* **1951**, *82*, 403−405. (b) Anderson, P. W.; Hasegawa, H. *Phys. Rev.* **1955**, *100*, 675−681. (c) De Gennes, P.-G. *Phys. Rev.* **1960**, *118*, 141−154.

(30) Bechlars, B.; D'Alessandro, D. M.; Jenkins, D. M.; Iavarone, A. T.; Glover, S. D.; Kubiak, C. P.; Long, J. R. *Nature Chem.* **2010**, *2*, 362−368.

(31) Loss, D.; Di Vincenzo, D. P. *Phys. Rev. A* **1998**, *57*, 120−126.

(32) (a) Wernsdorfer, W. In *Handbook of Magnetism and Advanced Magnetic Materials*; Wiley: New York, 2007. (b) Bogani, L; Wernsdorfer, W. *Nat. Mater.* **2008**, *7*, 179−186.

(33) Sonchini, A.; Mallah, T.; Chibotaru, L. *J. Am. Chem. Soc.* **2010**, *132*, 8106−8114.

(34) Polinger, V. *Adv. Quantum Chem.* **2003**, *44*, 59−88.

(35) Jung, Y.; Silbey, R. J.; Cao, J. *J. Phys. Chem. A* **1999**, *103*, 9460−9468.

(36) (a) Belinsky, M. I. *Mol. Phys.* **1987**, *60*, 793−819. (b) Belinsky, M. I. *Chem. Phys.* **2003**, *291*, 1−25.